

**Yousuf Mohamed-Ahmed**

**Non-contact heart rate  
estimation from video**

Computer Science Tripos - Part II

Gonville & Caius College

March 4, 2020



# Proforma

Name:	<b>Yousuf Mohamed-Ahmed</b>
College:	<b>Gonville &amp; Caius College</b>
Project Title:	<b>Non-contact heart rate estimation from video</b>
Examination:	<b>Computer Science Tripos - Part II, July 2020</b>
Word Count:	<b>0<sup>1</sup></b>
Project Originator:	Dr R. Harle
Supervisor:	Dr R. Harle

## Original Aims of the Project

## Work Completed

## Special Difficulties

None.

---

<sup>1</sup>This word count was computed by the **TeXcount** script

## **Declaration**

I, Yousuf Mohamed-Ahmed of Gonville & Caius College, being a candidate for Part II of the Computer Science Tripos, hereby declare that this dissertation and the work described in it are my own work, unaided except as may be specified below, and that the dissertation does not contain material that has already been used to any substantial extent for a comparable purpose.

Signed Yousuf Mohamed-Ahmed

Date March 4, 2020

# Contents

<b>1</b>	<b>Introduction</b>	<b>1</b>
1.1	Motivation . . . . .	1
1.2	Related work . . . . .	1
<b>2</b>	<b>Preparation</b>	<b>3</b>
2.1	Relevant computer vision techniques . . . . .	4
2.1.1	Face detection . . . . .	4
2.1.2	Optical flow . . . . .	4
2.1.3	Harris corner detection . . . . .	4
2.2	Approaches to signal processing . . . . .	4
2.2.1	Independent Component Analysis . . . . .	4
2.2.2	Fourier transforms . . . . .	4
2.3	Sensing and photoplethysmography (PPG) . . . . .	4
2.4	Remote photoplethysmography (rPPG) . . . . .	4
2.5	Languages and tooling . . . . .	4
2.5.1	OpenCV . . . . .	4
2.5.2	Mobile Vision API . . . . .	4
2.5.3	Python . . . . .	4
2.5.4	Kotlin . . . . .	4
2.5.5	Android . . . . .	4
2.6	Starting Point . . . . .	4
2.7	Requirements analysis . . . . .	4
2.8	Professional practice . . . . .	4
<b>3</b>	<b>Implementation</b>	<b>5</b>
3.1	Overview . . . . .	5
3.2	System design . . . . .	5
3.3	Face detection . . . . .	7
3.3.1	Face tracking . . . . .	7
3.4	Region selection . . . . .	10

3.4.1	Skin detection . . . . .	10
3.4.2	Improving the previous approaches . . . . .	14
3.5	Heart rate isolation . . . . .	18
3.5.1	Blind-source separation . . . . .	19
3.5.2	Identifying the heart rate . . . . .	21
3.6	Repository overview . . . . .	22
<b>4</b>	<b>Evaluation</b>	<b>23</b>
4.1	Face tracking . . . . .	23
4.2	Region selection . . . . .	23
4.2.1	Skin tone detection . . . . .	23
4.3	Heart rate isolation . . . . .	24
4.3.1	Pulse isolation . . . . .	24
4.3.2	Heart rate identification . . . . .	24
4.3.3	Window and stride size . . . . .	24
4.4	Evaluation method . . . . .	24
4.4.1	Experimental setup . . . . .	24
4.4.2	Ethics . . . . .	24
4.5	Capabilities of remote heart rate sensing . . . . .	24
4.5.1	Accuracy . . . . .	24
4.5.2	Energy consumption . . . . .	24
4.5.3	Time cost . . . . .	25
4.6	Summary . . . . .	25
<b>5</b>	<b>Conclusion</b>	<b>27</b>
	<b>Bibliography</b>	<b>29</b>
<b>A</b>	<b>Project Proposal</b>	<b>31</b>

# Chapter 1

## Introduction

### 1.1 Motivation

Optical heart rate monitors, the kind of which are standard in modern wearables, work by measuring the amount of light emitted by the surface of the skin. Given this signal, a heart rate can be extracted by analysing the predominant frequencies, for example, through the use of a Fourier transform.

This notion, can be extended to traditional cameras such as those present in smartphones.

### 1.2 Related work







## Chapter 2

# Preparation

### 2.1 Relevant computer vision techniques

#### 2.1.1 Face detection

#### 2.1.2 Optical flow

#### 2.1.3 Harris corner detection

### 2.2 Approaches to signal processing

#### 2.2.1 Independent Component Analysis

#### 2.2.2 Fourier transforms

### 2.3 Sensing and photoplethysmography (PPG)

### 2.4 Remote photoplethysmography (rPPG)

### 2.5 Languages and tooling

#### 2.5.1 OpenCV

#### 2.5.2 Mobile Vision API

#### 2.5.3 Python

#### 2.5.4 Kotlin

#### 2.5.5 Android

### 2.6 Starting Point

# Chapter 3

## Implementation

### 3.1 Overview

Abstractly, the program consists of three distinct tasks, each of which rely on the result from the previous. Together, forming a kind of pipeline:

- **Face detection:** identify a face in each supplied camera frame
- **Region selection:** given a bounding box around a face, select some set of pixels to consider which are amenable to heart rate detection
- **Heart rate isolation:** given a time series of the mean colour of some region of the face, infer the heart rate

Face detection is largely a solved problem and thereby the project mostly concentrates on the latter two, for which, there is very much ongoing research.

### 3.2 System design

Each of these tasks occur at different rates and, thereby, have different performance constraints which must be upheld. Face detection and region selection operate on every frame received from the camera and so must run in real-time, or risk dropping streamed frames.

Heart rate isolation, however, is only executed after some adequate number of data points is received and is recomputed after a fixed time. Since none of the prior stages rely on the estimated heart rate, its execution time requirements are less stringent. This is exploited to perform relatively expensive analyses without slowing earlier stages. Crucially, this relies on the assumption that it

can be run concurrently from the earlier stages. Separating these tasks allows for this concurrency to be implemented safely.

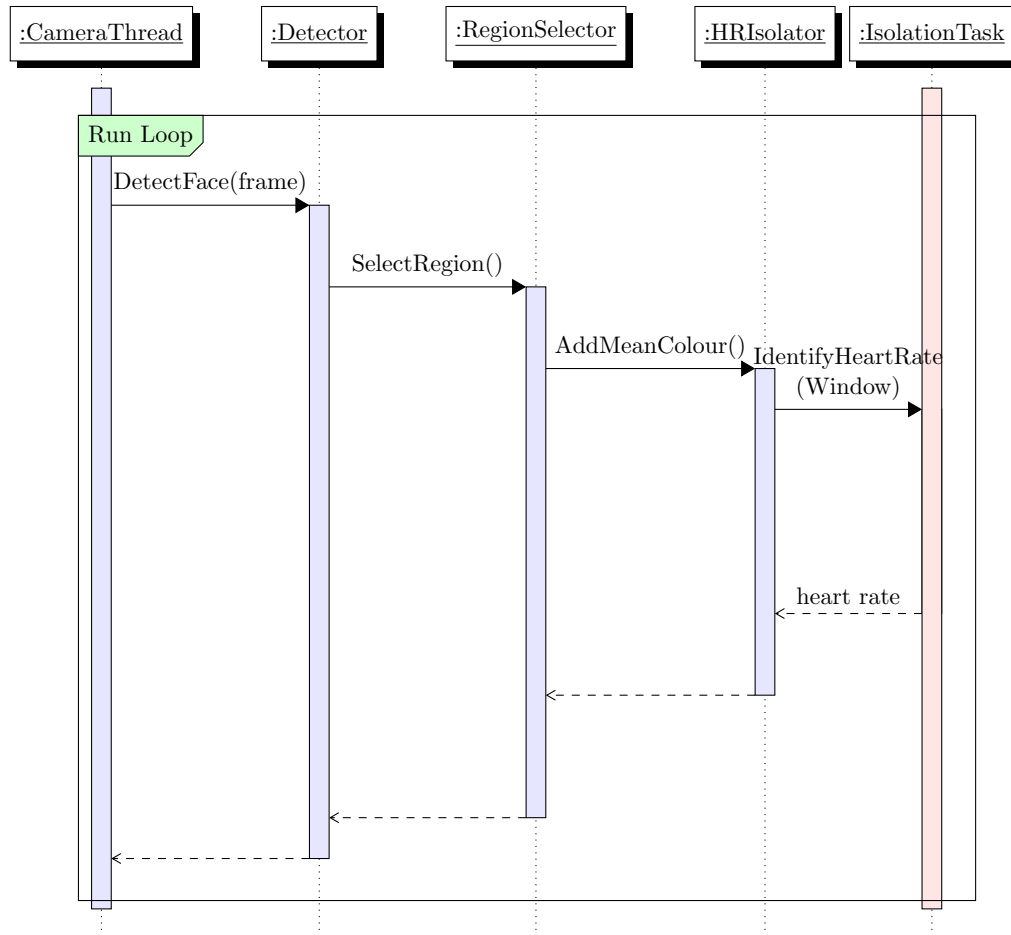


Figure 3.1: A diagram representing the design of the system

The camera streams frames to the **FaceDetector**. The **RegionSelector** then takes the mean pixel colour of the region considered and adds this value to the dataset. Once enough values have been collected, as defined by the window size, the **HRIsolator** spawns a new thread, the **IsolationTask**, which attempts to infer the heart rate from the window of values.

Although the region selection could also be executed in a separate thread, the associated setup costs are likely to have an adverse impact on real-time performance. However, one might wish to use more expensive region selection algorithms which cannot run in real-time. In these scenarios, the program could copy the frame and execute the selection in a separate thread from the main face detection loop. This is fundamentally a tradeoff between memory usage

and execution time. Furthermore, since there are only a finite number of threads which can be spawned, quickly the limit might be reached without providing much additional computation time to the **RegionSelector**. As a result, the **FaceDetector** and **RegionSelector** operate sequentially in the same thread.

### 3.3 Face detection

A face detector is expected to take a single frame and return a bounding rectangle within which a face is present. This could be extended to work on a stream of frames, naïvely, by simply repeated applying this face detector to each frame independently.

#### 3.3.1 Face tracking

Smartphone cameras can readily stream at high framerates, so it is unlikely that a face moves very much between a pair of consecutive frames. At sixty frames per second, frames are recorded only 0.017s apart. The position of the face in the previous frame, gives a strong indication of its subsequent position. Thus, there is opportunity for optimisation beyond simply applying a face detector to each frame individually. This is important since a speedup in this part of the pipeline provides opportunity for more expensive computation in subsequent stages which might improve accuracy. However, it is critical that any optimisations are resistant to motion. Using information from previous frames forms the distinction between face *detection* and *tracking*.

#### Point tracking

The key principle behind face tracking is to use information from previous frames to reduce the cost of subsequent face detections. To that end, I implemented an optical-flow based algorithm that tracks points on the face rather than repeatedly calling the face detector. The Lucas-Kanade algorithm [1], a particular variant of optical-flow, tracks a set of points between consecutive frames. Naturally, over time, these points will diverge from their true positions. This is because images contain large numbers of pixels with similar illumination, over time, these cannot be distinguished perfectly. When this occurs, the position of the face should be redetected.

Knowing when the points have diverged is non-trivial, since the true location of the face is unknown. It is crucial for any implementation to act safely

enough that the face is not lost track of, whilst simultaneously minimising the number of redetections. There are two obvious approaches to combat this. The algorithm could redetect the face:

- periodically
- when the tracked face changes in size significantly.

The former wastes computation time for stationary videos where the redetections might be unnecessary. Simultaneously, the time between redetections must be short enough to deal with videos with significant movement. This static approach, therefore, was not considered. For this reason, the latter was implemented. We track the face and if the size of the box surrounding it changes significantly, indicating that our confidence in the tracked points has reduced, then we recompute the true position of the face.

```

points = []
last_detection = None
def face_tracker(frame):
    if redetect or points is empty:
        face = face_detector(frame)
        last_detection = face
        points = select_new_points(face)
    else:
        points = track_points(points)
        face = bounding_box(points)
    redetect = change_in_size(last_detection, face) > threshold
    previous_face = face
    return face

```

Figure 3.2: A simplified pseudocode representation of an optical-flow based face tracker

**Impact of the rate of redetections** It is important to reason about precisely when face tracking provides a performance boost. To understand this let us consider a sequence of frames which the face tracker has been applied to. The cost of tracking is compared with that of repeatedly detecting the face in each frame independently. Under the following notation:

- $W$ : number of consecutive frames considered

- $R$ : the total number of redetections by the face tracker
- $n$ : size of each frame in pixels
- $p$ : number of points tracked
- $f(n)$ : cost of a face detection on a single frame of size  $n$
- $s(p, f)$ : cost of selecting  $p$  points to track in a face of size  $f$
- $g(p, n)$ : cost of tracking  $p$  points in a frame of size  $n$

The cost of the repeated face detector is  $Wf(n)$ . Since, for each frame in the sequence, it detects the face independently and incurs a cost of  $f(n)$ .

The point tracking approach instead has a cost of  $Wg(p, n) + R(f(n) + s(p, f))$ . For each redetection it calls the face detector and selects a new set of points. It also tracks the set of points for every frame, hence the term  $Wg(p, n)$ . In the worst case,  $R = W$ , so there is no saving in terms of computational complexity. Instead let us investigate for what values of  $R$  there is a cost saving.

$$\begin{aligned}
 Wf(n) &> Wg(p, n) + R[f(n) + s(p, f)] \\
 R &< \frac{W[f(n) - g(p, n)]}{f(n) + s(p, f)} \\
 \frac{R}{W} &< \frac{f(n) - g(p, n)}{f(n) + s(p, f)}
 \end{aligned}$$

Notice that  $R/W$  represents the percentage of frames for which a redetection occurs. There is only a performance saving when this percentage falls below the value on the right hand side. Furthermore, this value itself is based on the relative costs of face detection and of selecting and tracking points. Implicitly, the algorithm assumes that the cost of tracking and selecting points is less than that of face detection, otherwise, this endeavour would be useless. This assumption is validated and the limit is evaluated experimentally in section 4.1. From this it is shown that even for videos with lots of movement, the value  $R/W$  falls below this limit and the inequality is satisfied.

**Details** To maximise the performance of the optical flow algorithm, selecting points randomly will not suffice. That is because, points which are particularly different to their neighbours, for example, are much easier to track. To achieve this, the Shi-Tomasi corner detection algorithm is used which returns some number of points satisfying this condition. Furthermore, for face tracking to

work properly, the points selected must span the entire face of the user. This is relatively easily enforced by mandating a minimum distance between each of the points selected and by selecting enough points.

It is conservative enough that the true position of the face is not lost, whilst still providing a 3x performance boost on the naive face detection approach. This is fully evaluated in section 4.1.

## 3.4 Region selection

Face detection systems, typically, return a bounding box, within which it is believed a face is present. However, naturally, the box will also contain pixels from the background of the image since faces are not, in general, perfectly rectangular.

These background pixels will not contain any information as to the underlying heart rate of the user. As a result, considering the entire bounding box will add unnecessary noise to the resulting signal which consists of the mean colour from each region considered in the sequence of frames. One approach might be to only consider skin pixels, however, robust, pose-invariant skin detection is a somewhat unsolved problem. Furthermore, it is unclear whether all skin pixels are equally useful. For example, it might be that cheeks contain greater predictive power than the nose. Several approaches are presented regarding this problem with associated algorithms that are evaluated in section 4.2.

### 3.4.1 Skin detection

Suppose that we wish only to consider skin pixels. An obvious approach might be to apply an edge detection algorithm to isolate the boundary between the face and the background. However, edge detection algorithms, like the Canny edge detector, tend to produce large numbers of irrelevant edges and so were not implemented.

#### Colour-based filtering

Considering that skin tones tend to fall within a certain range of colours, one might encode this information in a primitive skin detector. For example, it is known that green is not a valid skin tone but brown might be. If a large enough number of skin tones are investigated then a range within which a skin pixel



might lie could be defined.

A dataset of  $\sim 250000$  skin and non-skin pixels was collected by Bhatt et al. [2] and was sampled across a variety of skin tones, genders and ages. One could define the range of skin tones present in this dataset as a rudimentary skin detector. Clearly this will fail in many scenarios but serves as a useful baseline for comparison with more advanced techniques.

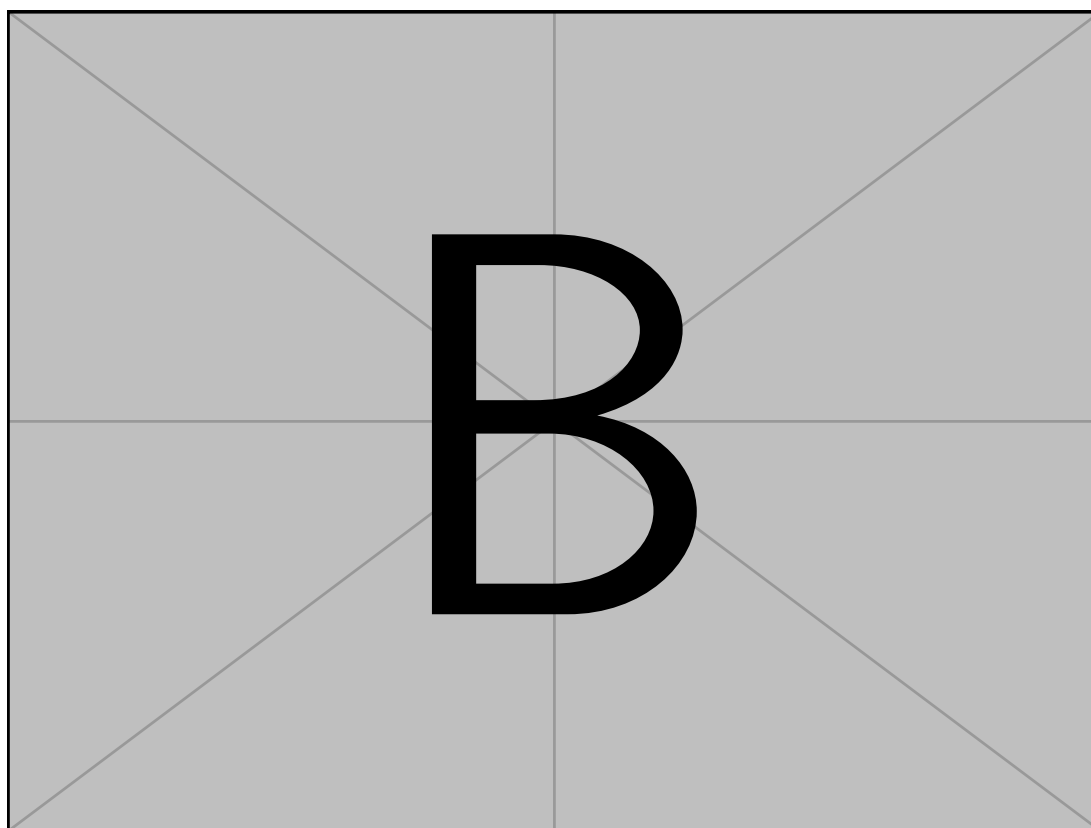


Figure 3.3: Skin dataset represented in YCbCr space

**Issues** This approach takes no consideration of the particular face that it is considering. Since it is not contextualised, it can fail in several circumstances. For example, there are some hair colours which could be a skin tone on another individual but are clearly not on the particular example in question. Instead, an algorithm should attempt to identify skin on the particular face in question.

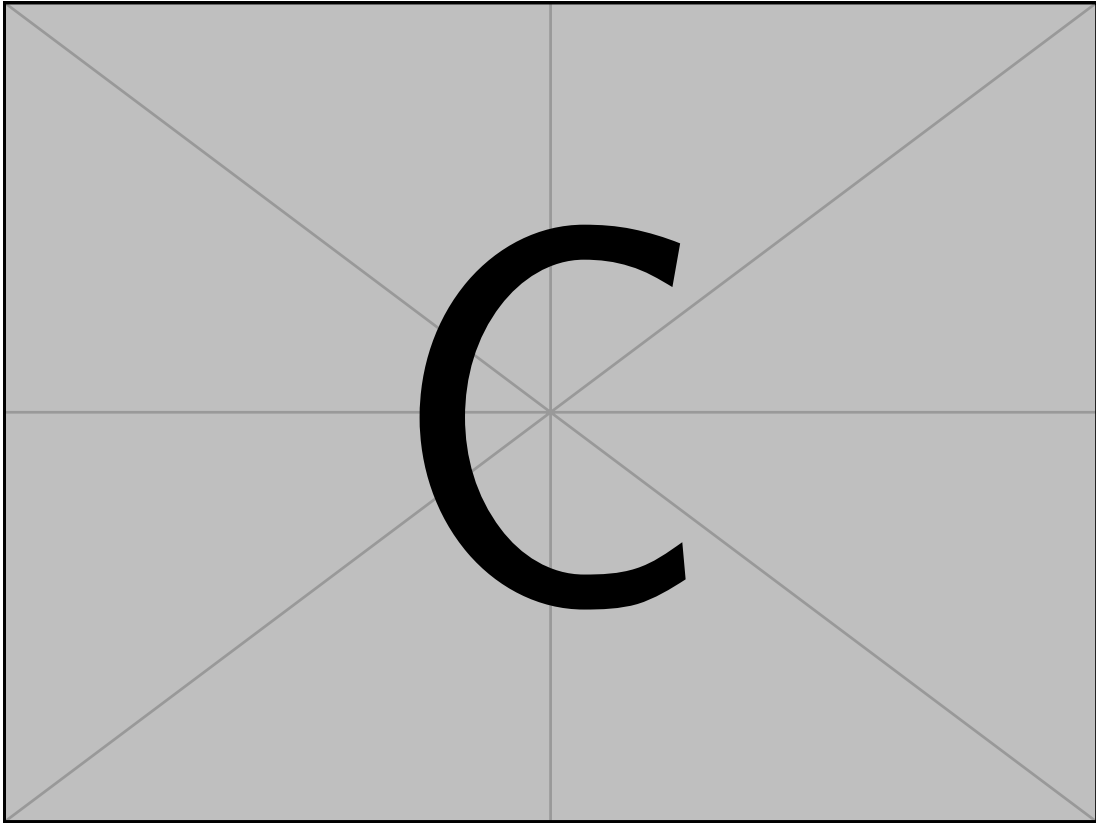


Figure 3.4: An example of the hair failure case

### K-Means

If we consider how a human might identify skin, it could involve initially identifying the skin tone of the person and then assuming all parts of the face of a similar colour are in fact skin. This reduces the problem to identifying the skin tone in a face and then measuring the colour difference between each pixel and the skin tone. If the colours are within some specified threshold, then we can consider them to be skin pixels.

We might suppose that the image consists of clusters of pixels, some of which belong to the skin and others which don't. The center of the cluster of skin pixels represents the skin tone of the individual. Implicitly, this approach assumes that the Euclidean distance between points in our colour space is representative of the perceived colour difference. This property is known as perceptual uniformity and is not a property of all colour spaces.

The colour space YCbCr is an approximation of perceptual uniformity

and hence the image is converted from RGB before the application of clustering. Under the assumption that our image consists of two clusters of pixels, skin and non-skin, we could simply apply the k-means algorithm to identify these clusters of pixels. Under the further assumption that the majority of pixels are skin pixels, we return the largest cluster as our set of skin pixels.

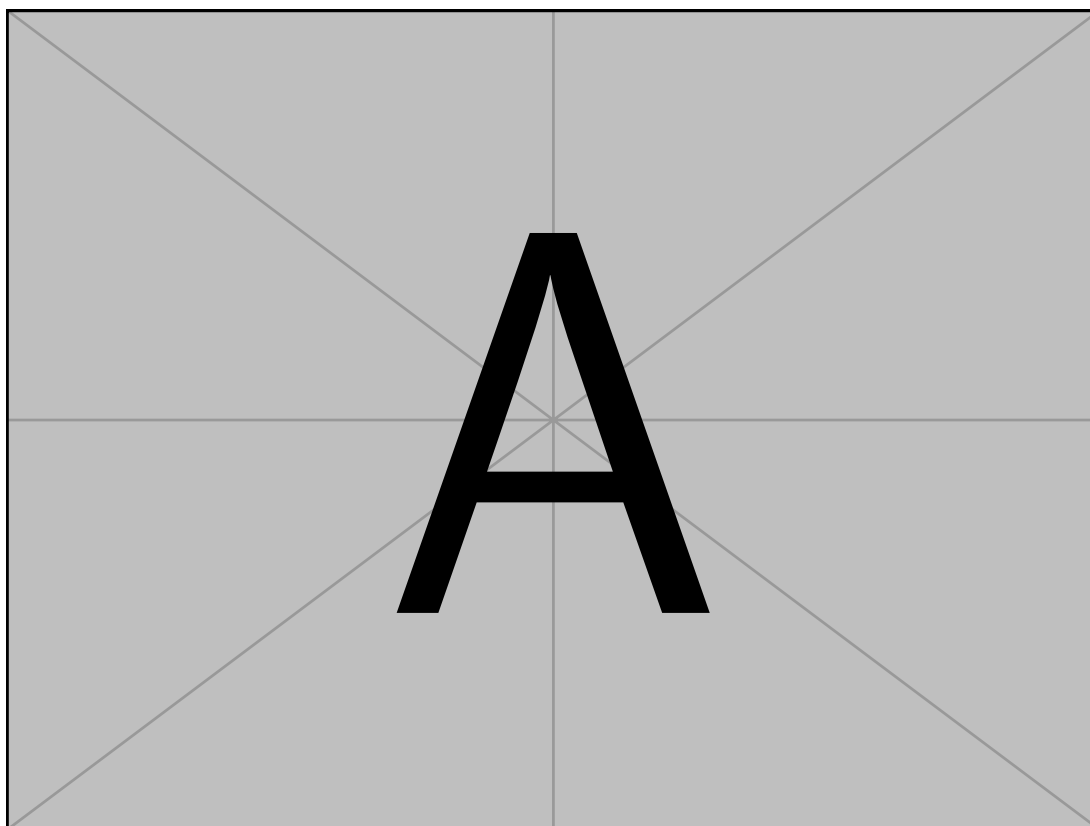


Figure 3.5: An example of the application of the k-means algorithm to skin detection

**Issues** The k-means algorithm, although it improves on the results of the rudimentary approach significantly, has a plethora of pitfalls.

- Location: since it encodes no notion of location with respect to other pixels, a lone pixel in the corner that has a similar colour to the skin tone is considered the same as a pixel surrounded by skin pixels
- Number of clusters: there's no rigorous means for deciding the number of clusters to expect in the data and the selection of this value is critical

- Performance: recall from Section 3.2 that, since the region selection operates on every frame, it must run in real-time. However, in benchmarking the k-means reference implementation in the SKLearn library takes an order of magnitude longer than the minimum requirement for this constraint.<sup>1</sup>

- Illumination resistance: the algorithm is not resistant to differences in illumination. For example, since there is no notion of location encoded, specular reflection on the forehead may not be considered as skin.

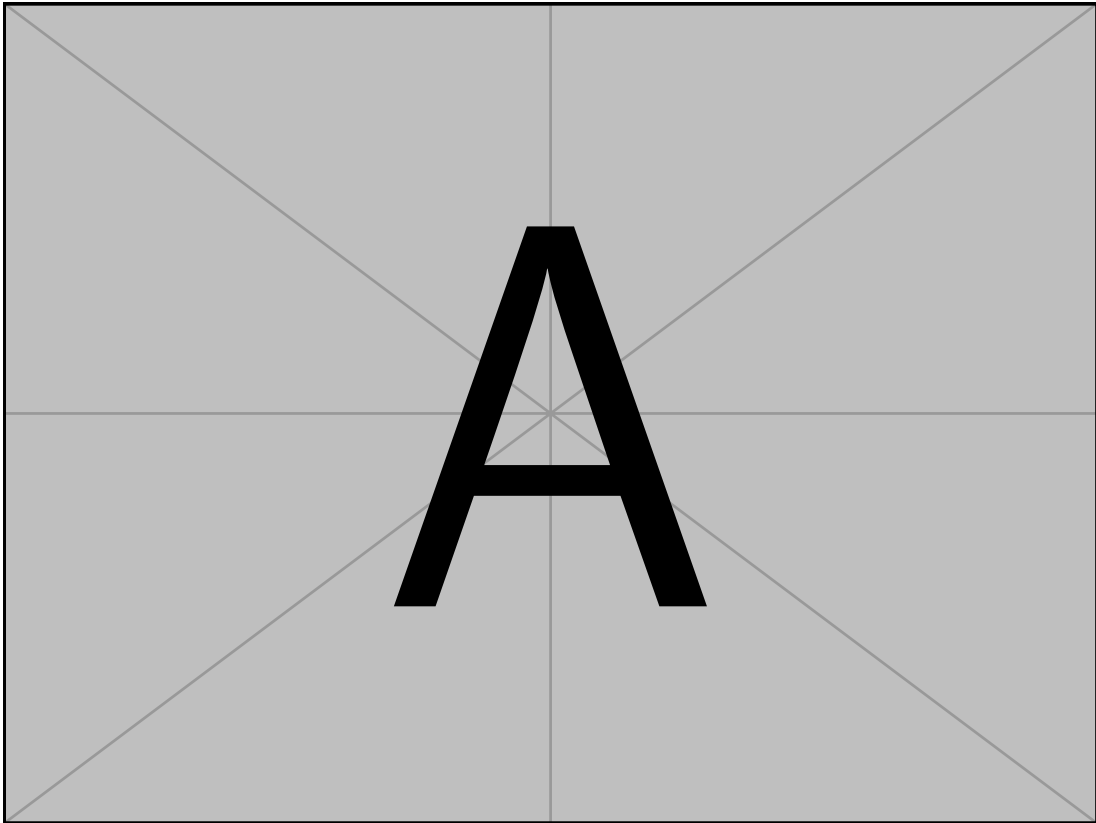


Figure 3.6: An example of the effect of differing the number of clusters

### 3.4.2 Improving the previous approaches

Recall that the purpose of the region selection is to return the mean colour of the pixels considered. The mean value from each frame is taken as a time series

<sup>1</sup>Suppose the camera streams at 30 frames per second, then each frame must be processed within 33ms, the reference implementation operates in the order of 100ms per frame.

which is used to infer the heart rate. So rather than attempting to classify each pixel as either skin or not, I use a combination of the previous techniques to take a weighted mean which emphasises pixels which are believed to be skin pixels, in such a way as to minimise the issues encountered with the previous techniques.

Instead of applying k-means to each frame, which is not feasible with the constraint of real-time performance, we apply it periodically. One of the resulting clusters will correspond to the skin tone of the face in question. Having identified the skin tone, this colour can be used as part of a probability model which we define to try and encode the likelihood of a particular pixel being part of the skin. This reduces the problem to:

- Use k-means to identify the skin tone
- Use the skin tone to identify skin in the face for some number of consecutive frames

### Identifying the skin tone

There are two expected properties of the cluster corresponding to the skin. It is likely to contain the largest number of pixels, since we'd expect most of the face to be composed of skin. It is also likely to fall within the range of expected human skin tones. The difficulty of this problem, however, is that neither of these properties are guaranteed to hold. For example, the face may be dominated by hair which could become the most prominent colour in the image. Likewise, changes in illumination or the presence of specular reflection might cause the skin tone of the face to be outside the expected range.

By considering both of these properties together, as a heuristic, it becomes more probable that the skin tone is identified correctly. I assign a score to each cluster,  $C$ , based on the number of elements in the cluster,  $|C|$ , and its distance from the expected range of skin tones,  $d_C$ .

$$\text{score}(C) = \alpha \cdot |C| - \beta \cdot d_C$$

The constants  $\alpha$  and  $\beta$  were selected experimentally. The skin tone is identified as the center of the cluster with the maximum score. This is shown to improve on simply selecting the largest cluster in Section 4.2.1.

### Identifying skin pixels using the skin tone

Identifying the skin tone, as described, requires the use of the k-means algorithm. However, as previously mentioned, this is not a particularly suitable algorithm for real-time applications. Thus, the skin tone can only be identified periodically rather than for every frame. So given the skin tone identified in some earlier frame, the value must be used to robustly detect skin pixels in subsequent frames. This is challenging since there will almost certainly be changing illumination conditions as well as changing positions of the skin pixels.

A possible approach could be to record the number of pixels that were in the skin cluster when the skin tone was identified. Then, our algorithm could select the  $n$  closest pixels in the colour space to the skin tone, where  $n$  was the number of pixels in the skin cluster. However, this would not be robust to rotations of the face, since, in subsequent frames, the number of pixels visible to the camera could change. Assuming a static value of  $n$  would not be robust.

Implicitly, the above solution also relies on the assumption that any change in illumination between frames affects all pixels equally. It assumes that in subsequent frames, the true skin pixels remain closer (in terms of Euclidean distance) to the skin tone than the non-skin pixels. This is a fairly strong assumption and is affected by phenomena such as shadows and specular reflection, which will, clearly, not affect all pixels equally. However, it is useful enough to make the problem more tractable than it was previously, without undermining the fidelity of the algorithm, if the skin tone is detected frequently enough. The validity of this assumption is made clear by the evaluation of the algorithm presented in Section 4.2.1. Therefore, we proceed by classifying pixels based on their Euclidean distance from the skin tone.

**A Bayesian approach** Recall that the first approach described classifies skin based on knowledge about the range of possible human skin tones. In this sense, it acts as a prior distribution, as, when classifying an individual pixel, it considers nothing of the face being presented. The k-means implementation, on the other hand, considers the face presented but it has no knowledge of the prior. It instead assumes that the largest cluster must be the set of skin pixels.

A natural way to combine these two approaches would be to consider the

problem of skin classification from a Bayesian perspective. Given some pixel  $x_i$  we want to discover the likelihood of it being a skin pixel, having been conditionalised on the skin tone of the person as well the colour of the pixel being classified. We have access to our prior distribution from the first approach, which indicates the likelihood of a particular colour being skin. Let us denote the following:

- $C_{\text{skin}}$  as the classification of a pixel as skin
- $x_i$  the colour of the pixel being considered
- $s$  the skin tone of the face

Given this notation the probability we wish to discover is precisely the following:

$$\Pr(C_{\text{skin}}|x_i, s)$$

Which, from Bayes' theorem, can be re-written as:

$$\frac{\Pr(C_{\text{skin}}, x_i, s)}{\Pr(x_i, s)} = \frac{\Pr(s|C_{\text{skin}}, x_i) \Pr(C_{\text{skin}}|x_i) \Pr(x_i)}{\Pr(x_i, s)}$$

We proceed with classification as follows, for some threshold probability  $t$  that defines the decision boundary:

$$\text{isSkin}(x_i) = \begin{cases} \text{True}, & \text{if } \Pr(C_{\text{skin}}, x_i, s) > t \\ \text{False}, & \text{otherwise} \end{cases}$$

**Defining the threshold** The most obvious selection would be to classify the pixel based on which class has the maximum posterior probability. That is the threshold value  $t$  would be  $\Pr(C_{\text{not-skin}}, x_i, s)$ , where  $C_{\text{not-skin}}$  is the class of pixels classified as not skin. In which case we would classify as follows:

$$\begin{aligned} \Pr(C_{\text{skin}}, x_i, s) &> \Pr(C_{\text{not-skin}}, x_i, s) \\ \frac{\Pr(s|C_{\text{skin}}, x_i) \Pr(C_{\text{skin}}|x_i) \Pr(x_i)}{\Pr(x_i, s)} &> \frac{\Pr(s|C_{\text{not-skin}}, x_i) \Pr(C_{\text{not-skin}}|x_i) \Pr(x_i)}{\Pr(x_i, s)} \\ \Pr(s|C_{\text{skin}}, x_i) \Pr(C_{\text{skin}}|x_i) &> \Pr(s|C_{\text{not-skin}}, x_i) \Pr(C_{\text{not-skin}}|x_i) \end{aligned}$$

Since we're assuming that there are only two possible classes, this is equivalent to:

$$\Pr(s|C_{\text{skin}}, x_i) \Pr(C_{\text{skin}}|x_i) > [1 - \Pr(s|C_{\text{skin}}, x_i)][1 - \Pr(C_{\text{skin}}|x_i)]$$

So an equivalent condition in only a single class is:

$$\Pr(s|C_{\text{skin}}, x_i) + \Pr(C_{\text{skin}}|x_i) > 1$$

**Defining probability distributions** Usually, one might attempt to learn these distributions from some relevant dataset. That is the prior distribution  $\Pr(C_{\text{skin}}|x_i)$  and the distribution  $\Pr(s|C_{\text{skin}}, x_i)$ . The prior  $\Pr(C_{\text{skin}}|x_i)$  was computed as the empirical distribution from the dataset discussed in Section 3.4.1. This dataset consists of randomly sampled pixels that are classified as skin or not, it does not include entire classified faces. Furthermore, to the best of my knowledge at the time of implementation, there are no such adequately sized datasets. Hence, attempting to learn the distribution  $\Pr(s|C_{\text{skin}}, x_i)$  was not deemed to be feasible.

As a result, a reasonable approach is to define the distribution  $\Pr(s|C_{\text{skin}}, x_i)$  based on the assumption that a skin pixel is likely close in colour to the overall skin tone. We want a function which returns a large probability if the Euclidean distance between the pixel and the skin tone is small. There are, however, an infinite number of functions which could encode this. The only requirements is that the probability of being a skin pixel is decreasing as a function of the distance between the colour of the pixel and the skin tone of the face.

A reasonable assumption might be that if the pixel being considered,  $x_i$ , is a skin pixel, then the skin tone,  $s$ , varies as a Normal distribution with mean  $x_i$ .

$$s \sim N(x_i, \sigma)$$

There is a finite range of possible values for the Euclidean distance between the colour of a pixel and the skin tone. This is because colours are discretised by the camera and therefore must lie between some set of bounds (usually 0 and 255). As a result, the defined distribution should also be discrete in nature.

### 3.5 Heart rate isolation

Given a time series of mean colours in the region of the frame considered, inferring the heart rate might, naively, be taken as the prevalent frequency. That is, the largest peak in the Fourier transform. However, it is important to consider that the colours observed are not only the result of the underlying



biological phenomenon of interest. Thereby this naive assumption is prone to returning, instead, the frequency of some other factor that impacts colour of the face. For example, respiration or movement of the face will have an impact, as well as any repetitive changes in lighting such as flickering. Isolating, the heart rate signal from the observed colour of the face, is a key part of the project.

To simplify this approach the problem is broken down into two subtasks:

- Identifying the pulse signal: given the noisy time series of observed colours for each frame, identify the signal corresponding to the pulse of the user
- Identifying the heart rate: given the pulse signal, identify the heart rate

Although, as will be explained, there is some overlap between the two to aide with correctly identifying the pulse.

### 3.5.1 Blind-source separation

Suppose that our observed colour signal,  $\mathbf{I}(t)$ , a vector-valued function, consists of a mixture of several underlying signals,  $x_i(t)$  one of which is the pulse,  $p(t)$ . Our observed signal exists in three dimensions (i.e. the particular colour space in use), is the result of the mixing of three underlying signals by some mixing matrix  $\mathbf{A}$ .

$$\mathbf{I}(t) = \mathbf{A} \begin{bmatrix} x_1(t) \\ x_2(t) \\ x_3(t) \end{bmatrix}$$

The nature of this task is to identify and return  $p(t)$  from only  $\mathbf{I}(t)$  and is known as the blind-source separation problem.

The above formulation is not enough to isolate the signal  $p(t)$ . Thus assumptions must be placed on the nature of each  $x_i(t)$  and  $p(t)$  in order to turn this into a tractable problem.

#### Independent components analysis (ICA)

A possible assumption might be that each of the  $x_i(t)$  are statistically independent. That is, informally, one cannot gain any information about one of these signals given an other. This assumption encodes the notion that the pulse, should be entirely independent from the other phenomena impacting the observed signal.

For example, suppose that the some of the  $x_i(t)$  are the result of some

physical phenomenon such as lighting conditions. In this case, it is intuitive to expect there to be no mutual information between the pulse and the other constituent signals. The ICA algorithm attempts to identify these signals based on this assumption, by using non-Gaussianity as a proxy for statistical independence.

Crucially, however, this approach returns the signals  $x_1(t)$ ,  $x_2(t)$  and  $x_3(t)$  but gives no indication regarding which signal corresponds to the pulse. In fact, the formulation of the ICA algorithm is such that each  $x_i(t)$  are returned in a random order. Thus some additional work must be undertaken to identify the pulse from the returned signal.

In this scenario, I proceed by attempting to identify the heart rate in each of these signals independently. This results in returning three different heart rate values, each of which has an associated power. This power value, which is the magnitude of the term in the Fourier transform associated with a given frequency, acts as a natural way of quantifying the importance of a particular frequency on the overall signal. Hence, I assume that the correct heart rate corresponds to whichever has the largest power. This particular assumption is evaluated in Section 4.3.1.

### Principal components analysis (PCA)

Alternatively, one might reframe the problem as finding a new orthogonal basis  $\mathbf{v}_1, \mathbf{v}_2, \mathbf{v}_3$  to represent each vector  $\mathbf{I}(t)$  in. The basis vectors are in the directions of maximal variance of the observed signal  $\mathbf{I}(t)$ . Finding these basis vectors is known as Principal Components Analysis.

In this scenario, we assume that the pulse occurs in the direction of most variance. Under the assumption that  $\mathbf{v}_1, \mathbf{v}_2, \mathbf{v}_3$  are in order from most to least variance, we return  $p(t) = \mathbf{I}(t) \cdot \mathbf{v}_1$ . Since we are only interested in the first basis vector, this is equivalent to fitting a plane to the three dimensional signal  $\mathbf{I}(t)$  that minimises the squared error. The resulting pulse signal is the projection of  $\mathbf{I}(t)$  onto this plane.

**Conclusion** The evaluation of these two algorithms reflects whether the assumption of statistical independence or maximal variance better reflects the issue of isolating the heart rate. The performance of these two approaches are evaluated in Section 4.3.1, from which it is concluded that ICA better serves the

requirements of heart rate isolation. Hence, it is concluded that the assumption of statistical independence is more valid.

### 3.5.2 Identifying the heart rate

Given a pulse signal, the heart rate corresponds to the average number of beats of the heart (seen as spikes in the signal) in a minute. A possible approach to identifying this is to simply count the number of peaks in the signal. The heart rate could also be taken as the most prevalent frequency in the Fourier transform, that is, specifically, the frequency with the largest associated power. Since the Fourier transform provides a particularly rich representation from which to identify the heart rate, the latter approach is used. For example, the Fourier transform enables easy analysis of the relative powers of different peaks present in the power spectrum, which would not be easily possible with the former approach.

#### The split peak issue

In practice, however, the true heart rate is not present in the resulting Fourier transform as a clear single peak. Instead, often, it will correspond to several peaks that are close by with smaller powers as is reported by van der Kooij et al. [3]. In order to avoid this, a Butterworth filter is applied which removes isolated peaks and increases the power of peaks close together as is recommended by van der Kooij et al. [3].

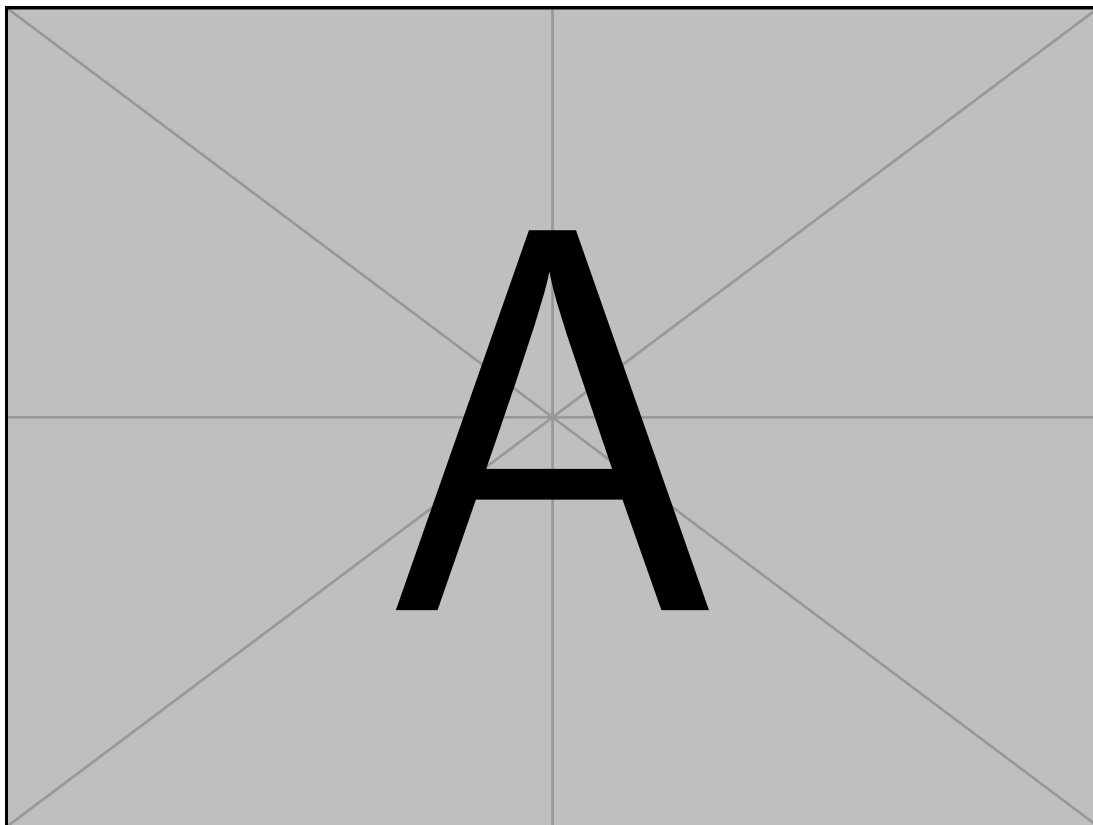


Figure 3.7: An example of the split peak issue with a Butterworth filter applied

## 3.6 Repository overview

# Chapter 4

## Evaluation

### 4.1 Face tracking

Research question

Metrics

Results

### 4.2 Region selection

Research question

Metrics

Results

#### 4.2.1 Skin tone detection

Research question

Metrics

Results

## 4.3 Heart rate isolation

### 4.3.1 Pulse isolation

### 4.3.2 Heart rate identification

### 4.3.3 Window and stride size

Research question

Metrics

Results

## 4.4 Evaluation method

### 4.4.1 Experimental setup

### 4.4.2 Ethics

## 4.5 Capabilities of remote heart rate sensing

### 4.5.1 Accuracy

Research question

Metrics

Results

### 4.5.2 Energy consumption

Research question

Metrics

Results

### 4.5.3 Time cost

Research question

Metrics

Results

## 4.6 Summary





# Chapter 5

## Conclusion



# Bibliography

- [1] Bruce D. Lucas and Takeo Kanade. An iterative image registration technique with an application to stereo vision (darpa), April 1981.
- [2] Abhinav Dhall Rajen Bhatt. Skin segmentation dataset. *UCI Machine Learning Repository*.
- [3] Koen M. van der Kooij and Marnix Naber. An open-source remote heart rate imaging method with practical apparatus and algorithms. *Behavior Research Methods*, 51(5):2106–2119, 2019.



# Appendix A

## Project Proposal

